DNase 1 Retains Endodeoxyribonuclease Activity Following Gold Nanocluster Synthesis

ARTICLE *in* ANALYTICAL CHEMISTRY · JULY 2014

Impact Factor: 5.64 · DOI: 10.1021/ac5005794 · Source: PubMed

4 AUTHORS, INCLUDING:

Abby L West
Army Research Laboratory
16 PUBLICATIONS **122** CITATIONS
SEE PROFILE

Mark H. Griep
Army Research Laboratory
53 PUBLICATIONS **185** CITATIONS
SEE PROFILE

analytical chemistry

Article

pubs.acs.org/ac

DNase 1 Retains Endodeoxyribonuclease Activity Following Gold Nanocluster Synthesis

Abby L. West,*[,†] Mark H. Griep,[†] Daniel P. Cole,[‡] and Shashi P. Karna[†]

[†]Weapons and Materials Research Directorate, U.S. Army Research Laboratory, ATTN: RDRL-WM, 4600 Deer Creek Loop, Aberdeen Proving Ground, Aberdeen, Maryland 21005-5069, United States

[‡]Vehicle Technology Directorate, U.S. Army Research Laboratory, ATTN: RDRL-VT, 4603 Deer Creek Loop, Aberdeen Proving Ground, Aberdeen, Maryland 21005-5069, United States

Supporting Information

ABSTRACT: Here we present the synthesis of the enzyme DNase 1 stabilized gold nanoclusters (DNase 1:AuNCs) with core size consisting of either 8 or 25 atoms. The DNase 1:Au_8NCs exhibit blue fluorescence whereas the DNase 1:Au_{25}NCs are red emitting. In addition to the intense fluorescence emission, the synthesized DNase 1:AuNC hybrid retains the native functionality of the protein, allowing simultaneous detection and digestion of DNA with a detection limit of 2 μg/mL. The DNase 1:AuNCs could be conveniently employed as efficient and fast sensors to augment the current time-consuming DNA contamination analysis techniques.

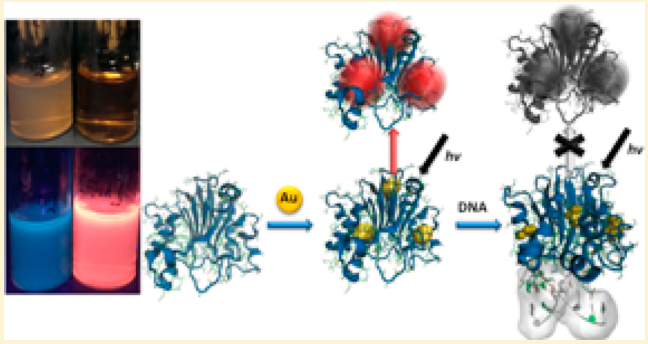

Noble metal nanoclusters (NCs) possess discrete energy levels and exhibit size tunable fluorescent emissions similar to semiconductor quantum dots (QDs) (Figure 1).[1−3]

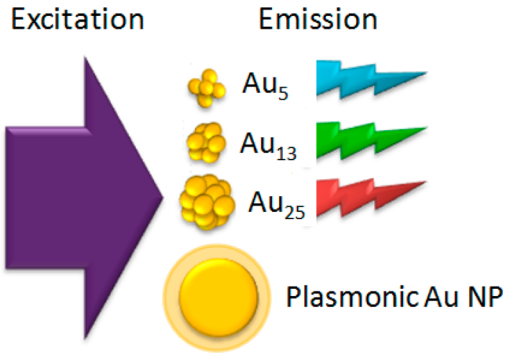

Figure 1. Comparison of distinct fluorescence emissions exhibited by gold nanoclusters to the plasmonic transitions of gold nanoparticles.

This is in contrast to metal nanoparticles (NPs), which do not exhibit fluorescence but show plasmonic transitions involving surface electrons. By definition, NCs are small clusters of metal atoms ranging from fewer than ten to several hundred atoms with a diameter of less than 2 nm.[2] In recent years, NCs have attracted a great deal of attention due to their unique optical properties, high degree of biocompatibility, and facile synthesis routes.[1,2,4−11]

Of particular interest are NCs synthesized and stabilized by biomolecules, specifically proteins (P-NCs) due to their highest level of biocompatibility and environmentally friendly synthesis routes. Recently, several proteins, such as bovine serum albumin (BSA),[12] apo-transferrin,[13] pepsin,[14] lysozyme,[15] insulin,[16] horseradish peroxidase,[17] and others, have been used to synthesize protein-stabilized NCs. In addition, some P-NCs, such as human apo-transferrin,[13] insulin,[16] and horseradish peroxidase,[17] have also been shown to retain native function, thus offering a multifunctional bio-nano hybrid system capable of simultaneous visualization and quantification of targeted biological process.[4,12−20]

Here, we present the synthesis and sensing application of DNase 1 stabilized gold nanoclusters (AuNCs). The nanoclusters consist of either 8 or 25 Au atoms and exhibit intense blue (Au_8) or red (Au_{25}) fluorescence emission, long-term stability, and resistance to photobleaching. Moreover, we show that the DNase 1:AuNC hybrid retains the native functionality of DNase 1 (Scheme 1).

EXPERIMENTAL METHODS

Nomenclature. DNase 1:AuNCs were synthesized with a variety of gold concentrations. To simplify the various reaction scenarios and product species, we will refer to the samples by the gold concentration used in the synthesis protocol. For example, 10 mM DNase 1:AuNCs will represent the blue emitting DNase 1:AuNCs that were synthesized with a final concentration of 10 mM $HAuCl_4$ in the reaction conditions, 0.5

Received: February 11, 2014
Accepted: July 4, 2014
Published: July 4, 2014

   dx.doi.org/10.1021/ac5005794 | Anal. Chem. 2014, 86, 7377−7382

Scheme 1. Schematic of the Formation of DNase 1:AuNCs and the DNA Mediated Quenching of NC Fluorescence

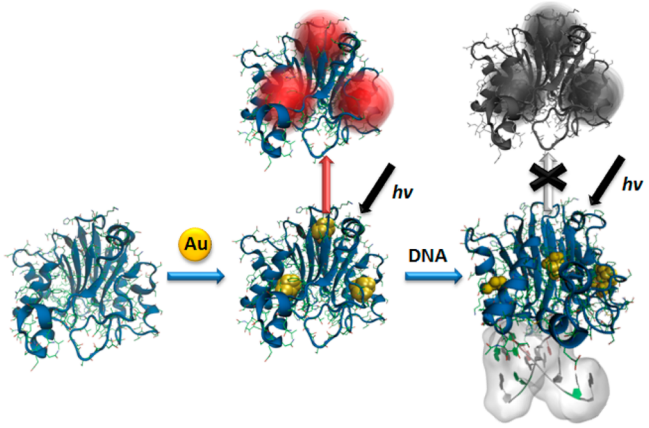

mM DNase 1 1:AuNCs will represent the red emitting protein−AuNC hybrid, and so on.

Synthesis of DNase 1 Stabilized AuNCs. DNase 1 from bovine pancreas (Sigma-Aldrich) was resuspended in Milli-Q water at a concentration of 20 mg/mL. Two milliliters of $HAuCl_4$(aq) (20, 10, 5, or 1 mM) was added to 2 mL of protein solution under vigorous stirring at 37 °C (Table 1).

Table 1. Representation of the Different AuNC Synthesis Conditions Examined in This Study

trial#	stock [protein] (mg/mL)	stock [Au] (mM)	final [Au] (mM)	1 M NaOH added (μL)
1	20	20	10	400
2	20	10	5	200
3	20	5	2.5	200
4	20	1	0.5	200

After 5 min, 200 μL of NaOH (1 M) was added to raise the pH to ∼12 for the 1, 5, and 10 mM $HAuCl_4$ samples whereas 400 μL of NaOH (1M) was required to obtain a pH of 12 for the 20 mM $HAuCl_4$ sample due to the increase concentration of gold ions. The increase in pH activates the reductive activity of the tyrosine residues within the protein. The various protein/gold mixtures were then left to react for 12 h. The solution changed in color from light yellow to various shades of deeper yellow/gold over the course of the reaction. A parallel experiment was set up with 20 mg/mL protein alone as a control. This solution was initially clear and remained so throughout the course of the incubation.

Ultraviolet−Visible (UV−Vis) Spectroscopy. Optical absorption and emission spectra of the synthesized DNase 1:Au NCs were measured with a Nanodrop 2000c UV−visible spectrometer over a wavelength range of 200 to 800 nm.

Fluorescence Spectroscopy. The fluorescence emission spectra were collected with a Horiba Jobin Yvon FluoroLog-3 spectrofluorometer with maximum excitation wavelengths of 365, 395, 450, and 488 nm. The emission spectrum was measured from 400 to 700 nm. The fluorescence excitation spectra were obtained through the measurement of two different maximum emission wavelengths, namely 460 and 640 nm.

X-Ray Photoelectron Spectroscopy (XPS) Analysis. Near-surface compositional depth profiling of the as-deposited coatings was performed using the Kratos Axis Ultra X-ray photoelectron spectroscopy system, equipped with a hemispherical analyzer. A 100 W monochromatic Al Kα (1486.7 eV) beam irradiated a 1 mm × 0.5 mm sampling area with a takeoff angle of 90°. The base pressure in the XPS chamber was held between 10^{-9} and 10^{-10} Torr. Elemental high resolution scans for Au_{4f} core level were taken in the constant analyzer energy mode with 160 eV pass energy. The sp^3 C_{1s} peak was used as reference for binding energy calibration.

Transmission Electron Microscopy. Morphological studies and elemental characterization of the materials were performed using a field emission transmission electron microscopy (TEM) instrument (JEOL JEM-2100F TEM/STEM) operated at 200 kV. The TEM system was equipped with an energy dispersive spectroscopy system (INCA 250, Oxford Instruments) and imaging filter (Gatan). Microscopy samples were prepared for analysis through the following steps: (i) bulk material was ground up using a mortar and pestle, (ii) particles were dispersed in deionized water and bath sonicated for 15 min, (iii) the solution was pipetted onto TEM grids (ultrathin carbon film on holey carbon support film, 300 mesh, Ted Pella, Inc.), followed by removal of excess solution using a filter paper, and (iv) samples were allowed to dry in air at room temperature for 2 h.

DNase 1 Activity Assay. All DNase 1 activity assays were completed in triplicate. A 1 kb double-stranded DNA (dsDNA) ladder with sizes ranging from 10 to 0.5 kb (New England Biolabs) was used as a substrate for cleavage by the enzyme endodeoxyribonuclease, DNase 1. Enzyme activity assays for both native DNase 1 and DNase 1:AuNCs were carried out in a final volume of 20 μL of buffer (100 mM sodium acetate, 6.25 mM magnesium sulfate pH 5.0), containing 2 μg of dsDNA. The reaction was incubated at room temperature for 20 min followed by the addition of 2 units of the control enzyme and 4 units of the various DNase 1:AuNC synthesis reactions. This reaction was further incubated for 30 min at 37 °C. After incubation, the reaction was heated at 99 °C for 1 min to deactivate the enzyme. The level of DNA degradation was analyzed by 2% agarose gel electrophoresis.

To determine the effect of DNA digestion on DNase 1:AuNC fluorescence, NC fluorescence was monitored during DNA addition. In a typical experiment, 300 mL of 20 mg/mL DNase 1:AuNCs in water was added to a 0.5 cm PL Spectrosil far-UV quartz window fluorescence cuvette (Starna Cells). The fluorescence spectrum of the NCs alone was obtained with an excitation wavelength of 390 nm (10, 5, and 0.5 mM Au(III)) or 490 nm (2.5 mM Au(III)). DNA from calf thymus (Sigma-Aldrich) was titrated and the change in fluorescence measured. The decrease in fluorescence at the max emission wavelength was plotted and fitted with a linear regression line.

RESULTS AND DISCUSSION

Traditional chemical reduction and polymer etching techniques for gold nanocluster synthesis require the addition of harsh and environmetally unfriendly reducing agents such as soduim borohydride and tetrabutylammonium borohydride.[3,7,8,21] These agents are necessary to reduce the Au(III) in solution to the final oxidation states of Au(I) and Au(0) that comprise the nanocluster. Ying and co-workers[12] were the first to use the theory of biomineralization to create a biostabilized AuNC using the amino acids within BSA as the exclusive reducing agent during NC synthesis. The amino acid tyrosine, which contain a phenolic group and residues with a pK_a value of 10.07, has the ability to reduce gold in an alkaline environ-

dx.doi.org/10.1021/ac5005794 | Anal. Chem. 2014, 86, 7377−7382

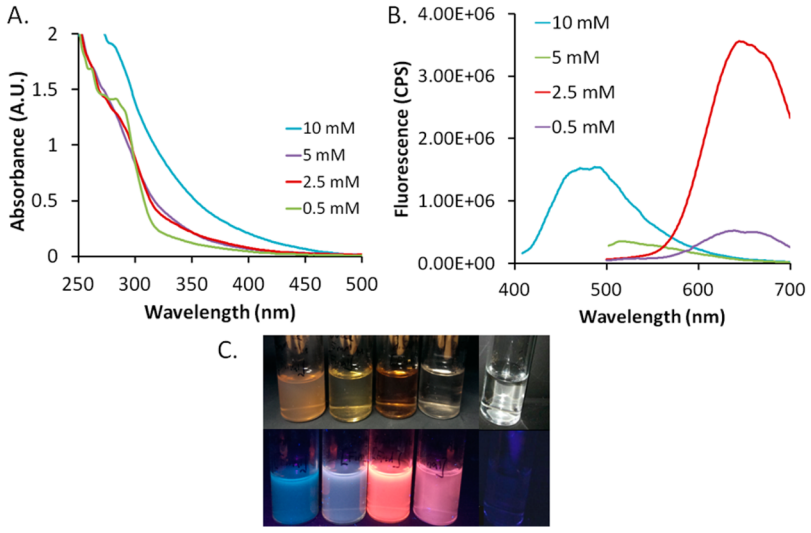

Figure 2. Fluorescence emission of DNase 1:AuNCs. (A) UV−visible spectra and (B) emission spectra for the different DNase AuNCs. (C) Visible (top) and UV (bottom) illumination of DNase AuNCs (From left to right: 10, 5, 2.5, 0.5, and 0 mM Au(III) added).

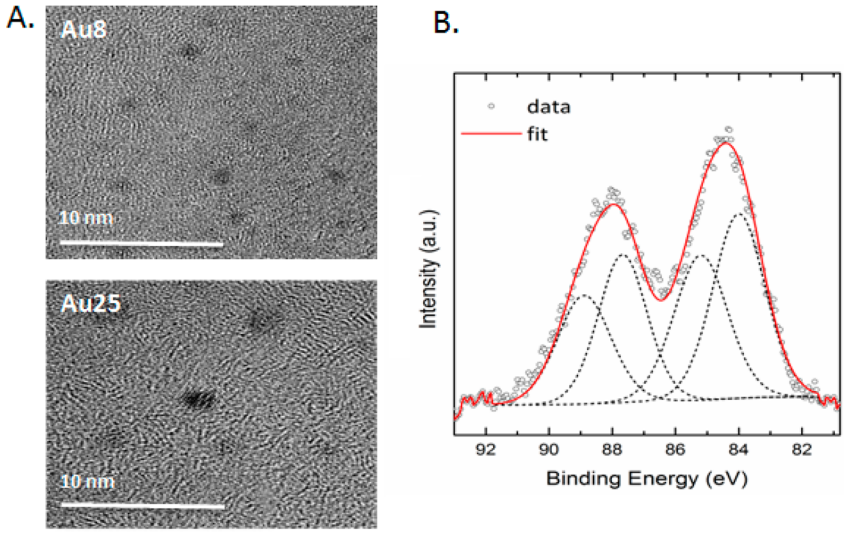

Figure 3. Physical characterization of DNase 1:AuNCs. (A) TEM images of DNase 1:Au_8NCs (top) and DNase 1:Au_{25}NCs (bottom). (B) XPS data for DNase 1:Au_{25}NCs. Au 4f spectra were fitted and confirm the presence of two distinct doublet Au 4f7/2 peaks at 84 eV and the other at 85.2 eV, corresponding to Au(0) and Au(I), respectively.

ment.[22] Therefore, raising the pH to ∼12 during synthesis ionizes the phenol and activates the reducing capability of these residues. As DNase 1 has 15 tyrosine residues, it is expected to serve as a good stabilizing agent for nanocluster synthesis. DNase 1 from bovine pancreas was used as the template for nanocluster synthesis in this study. Gold nanocluster encapsulation by DNase 1 was completed after 12 h of incubation at 37 °C. The size of the resultant nanocluster was dependent upon the initial Au(III) concentration used in the synthesis reaction.

Gold(III) Concentration-Dependent Synthesis of DNase 1 Stabilized AuNCs. DNase 1 stabilized AuNCs with varied peak emission wavelengths were synthesized by incubating 20 mg/mL enzyme with a range of Au(III) from 10 to 0.5 mM final concentration. After a subsequent raise in pH and 12 h incubation time, DNase 1 stabilized AuNCs with blue, gray, red, and pink fluorescence could be observed with UV illumination from the 10, 5, 2.5, and 0.5 mM $HAuCl_4$ reactions, respectively (Figure 2b,c). The reaction products that emit strong blue and red fluorescence are thought to be homogeneous solutions of DNase 1 stabilized $Au_{5/8}$ and Au_{25} nanoclusters. As gray and pink are not true fluorescent colors, we hypothesized that the gray and pink emitting samples are some form of reaction intermediate resulting from nonideal reaction conditions (data not published) and chose to not continue study with these two reaction products and focus on the homogeneous blue and red emitting samples.

Photophysics of DNase 1 Stabilized AuNC. The UV−visible and fluorescence emission spectra of the blue and red emitting clusters are shown in Figure 2. As seen from the figure, the blue emitting clusters synthesized with 10 mM Au(III) exhibit the maximum emission wavelength at 460 nm and the maximum excitation wavelength at 395 nm when monitoring the 460 nm peak fluorescence. Both the excitation and emission spectra were clearly pure and contain no other peaks (see the Supporting Information, Figure S-1). According to the study presented by Kawasaki et al.[14] involving the pH-dependent synthesis of blue, green, and red emitting AuNCs, a peak

dx.doi.org/10.1021/ac5005794 | Anal. Chem. 2014, 86, 7377−7382

emission wavelength of 460 nm is consistent with gold clusters composed of eight atoms. The emission maximum at 460 nm is also consistent with data for Lysozyme-stabilized Au_8 clusters reported by Chen and Tseng.[23]

The Red emitting clusters synthesized with 2.5 mM Au(III) exhibit peak fluorescence at 640 nm with a maximum excitation wavelength of 460 nm. Similar to the blue emitting clusters, the emission spectrum of the red fluorescent clusters possesses high purity with a small contaminating peak at 460 nm. The emission wavelength of our DNase 1:AuNCs compares well with previously reported Au_{25}NCs stabilized with BSA (λem = 640 nm),[12] Lysozyme (λem = 657 nm),[15] horseradish peroxidase (λem = 650 nm),[17] and pepsin (λem = 640 nm).[14] The photostability of AuNCs is limited by the inherent stability of the stabilizing protein. As DNase 1 is a soluble, nonmembrane associated enzyme, its stability is quite high, remaining stable at room temperature for 48 h and at 4 °C for more than 2 months. As expected, the stability of all of the DNase 1:AuNC synthesis products is very high and reflects the stability of the stabilizing enzyme. The samples retained the same emission spectra for more than 2 months at 4 °C and for 48 h at ambient temperature (data not shown).

Physical Properties of DNase 1 Stabilized AuNCs. The red and blue emitting DNase 1:AuNCs were characterized by both high-resolution tunneling electron microscopy (HR-TEM) and XPS to determine the size and oxidation states of the clusters. The HR-TEM data for the blue emitting clusters showed a homogeneous population of subnanometer to 1 nm clusters (Figure 3A, top). These results are in agreement with previously published data for the lysozyme and pepsin stabilized Au_8 clusters.[14,23] Comparison of the HR-TEM data for the red emitting DNase 1:AuNCs (Figure 3A, bottom) to other known protein stabilized Au_{25}NCs such as BSA,[12] pepsin,[14] lysozyme,[15] and apo-transferrin[13] showed very high similarity. These data lend further support to the blue and red emitting DNase:AuNCs being composed of 8 and 25 atoms, respectively. Following HR-TEM analysis, XPS was conducted to determine the ratio of Au(I) ions the form the shell of the clusters and Au(0) that forms the core of the cluster. The ratio of Au(I) to Au(0) should decrease as the cluster core size increases (i.e., from Au_8 to Au_{25}).[14,23] For example, lysozyme Au_8 clusters are completely composed of elemental gold (Au(0)) with no Au(I) present on the surface.[23] As such, the DNase 1:Au_{25}NCs should have a higher percentage of oxidized metal than the DNase 1:Au_8NCs. As shown in Figure 3B, the DNase 1:Au_{25}NC XPS spectra of Au 4f spectra were fitted and confirm the presence of two distinct doublet Au 4f7/2 peaks at 84 eV and the other at 85.2 eV, corresponding to Au(0) and Au(I), respectively, and show a higher percentage of Au(I) than elemental metal, as expected. However, we were unable to successfully acquire XPS spectra of the DNase 1:Au_8NCs. It is possible that the XPS instrument we were using was unable to resolve the small clusters or that the sample degraded upon X-ray exposure.

Enzymatic Activity of DNase 1:AuNC Hybrids. One of the most attractive aspects of using biomolecules to synthesize and stabilize fluorescent nanoclusters is their applications in biospecific processes. This requires preserving of the native functionality of the biomolecules. In the past, several of the proteins that have been demonstrated to synthesize gold nanoclusters have also been shown to retain native activity after the synthesis process. For example, the iron transport and storage protein transferrin retains iron binding and transport capability following Au_{25} nanocluster synthesis.[13] In addition, the enzyme horseradish peroxidase has also been demonstrated to retain the ability to oxidize various substrates after Au_{25}NC synthesis and thus has been used as a hydrogen peroxide sensor. The enzyme DNase 1 is an endodeoxyribonuclease that is responsible for the degradation (cleavage) of double-stranded DNA (dsDNA) to a smallest unit of four base pair segments. To examine the endodeoxyribonuclease activity of the 8 and 25 atom DNase 1:AuNCs synthesized in the present study, the clusters were incubated with a standard 1 kb dsDNA ladder and the reaction products were analyzed on an agarose gel (Figure 4). As a control, the dsDNA was also incubated with the pure enzyme (DNase 1). Figure 4 shows the results of the agarose gel electrophoresis, where lane 1 is for dsDNA alone and lane 2 shows the column for ds DNA and pure enzyme, DNase 1. Lanes 3 and 4, respectively, show the columns for dsDNA +DNase 1:Au_8 and dsDNA+DNase 1:Au_{25}. As is clear from the gel-electrophoresis columns, both of the DNase 1 stabilized gold nanoclusters were able to degrade the dsDNA template (Figure 4, lanes 3 and 4). Although, neither of the DNase 1:AuNCs are able to degrade dsDNA to the degree of the control (pristine) enzyme shown in lane 2, which can be seen from the bright smearing in lanes 3 and 4, due to larger dsDNA fragments observed on the gel, and no such smearing for the enzyme alone. there is significant degradation of dsDNA as very little of the bands from the intact ladder are visible. One can clearly see such bands of the intact dsDNA in unreacted sample (lane 1).

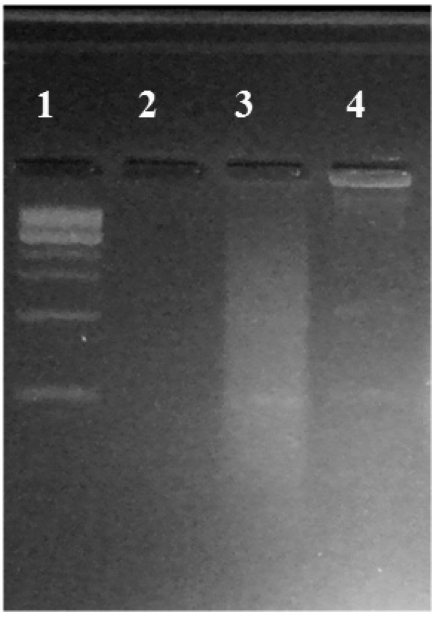

Figure 4. DNase 1 activity assay. Lane 1: blank reaction with dsDNA marker alone. Lane 2: control reaction with stock DNase 1. Lanes 3 and 4: test reaction with the DNase 1 stabilized Au_8 and Au_{25} clusters. All of the DNase 1:AuNC synthesis products are able to degrade dsDNA.

It is also interesting to note that each of the DNase 1:AuNC complex, regardless of the size of the Au clusters (Au_8 or Au_{25}) sppears to degrade dsDNA to the same degree. This is somewhat surprising, since one can expect that the smaller cluster (Au_8), with less propensity to induce structural changes in the stabilizing enzyme would allow a higher degree of enzymatic activity than the larger (Au_{25}) clusters. However, our

dx.doi.org/10.1021/ac5005794 | Anal. Chem. 2014, 86, 7377−7382

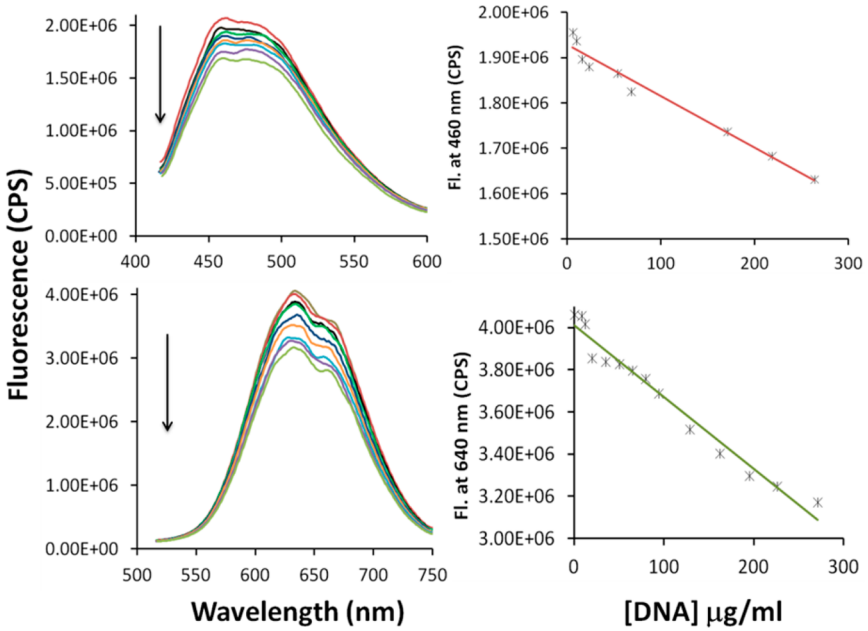

Figure 5. Left panel: fluorescent responses of DNase 1:Au_8NCs (top) and DNase:Au_{25}NCs (bottom) after the addition of DNA (2−260 μg/mL). Right panel: plot of the fluorescence decrease at 460 or 640 nm for the Au_8 and Au_{25} clusters, respectively.

results clearly demonstrate that, at least between the Au_8 and Au_{25} clusters there is no real difference in the enzymatic activity of the stabilizing protein. To date, all of the studies on the native activity of the AuNC stabilizing proteins have been focused on cluster sizes of 25 atoms. To the best of our knowledge, the present study is the first to demonstrate retained native enzymatic activity of the stabilizing enzyme following the synthesis of Au_8NCs and practically no effect of the size (Au_8 vs Au_{25}) of the metal NCs on the enzymatic activity of DNase 1.

We next sought to examine the effect of the biocatalytic activity of the enzyme on the fluorescence characteristics of the synthesized NCs and to determine if the detectable limit varied between the different synthesis products. For practical detection of dsDNA, the digestion of dsDNA by DNase 1:AuNCs must produce a quantifiable change in fluorescence. Such a change in fluorescence following substrate addition has previously been demonstrated with horseradish peroxidase stabilized AuNCs, wherein a linear decrease in NC fluorescence was observed upon titration of the substrate, hydrogen peroxide.[17] As the Au_8 clusters are smaller in size and therefore stabilized by fewer ligands, one could expect that changes in the protein environment and subsequent changes in ligand to cluster interactions could more greatly affect nanocluster fluorescence. Thus, one would expect the DNase 1:Au_8NC system to exhibit greater sensitivity in the detection assays. Surprisingly, we were unable to observe a difference in the detection limit between the DNase 1 stabilized Au_8 clusters and the Au_{25} clusters, both clusters show a marked decrease in fluorescence upon the addition of 2 ng/μL of DNA (Figure 5). The subsequent addition of DNA results in further quenching of NC fluorescence in a linear fashion. Interestingly, the DNase 1:AuNC synthesis products resulting in mixed clusters (5 and 0.5 mM Au(III)) also demonstrate fluorescence quenching upon the addition of 1 μg of DNA. As DNA can also serve as a biomolecular host for AuNC synthesis, a control experiment was conducted wherein 300 ng/μL (150 μg total) of DNA was added to a solution of BSA:Au_{25}NCs and no fluorescence quenching was observed for the BSA:Au_{25}NCs upon the addition of DNA (see the Supporting Information, Figure S-3). Clearly, the DNA mediated quenching of DNase 1:AuNC fluorescence was indeed caused by the substrate/enzyme interaction between DNA and DNase 1.

DNA contamination has long been recognized as a major problem in quantitative reverse transcriptase polymerase chain reaction (qRT-PCT) based studies, where pure solutions of template RNA are required.[24−27] Nevertheless, current techniques for the isolation of RNA from cells, both prokaryotic and eukaryotic, have been shown to contain a significant amount of DNA contamination with concentrations ranging anywhere from 1 to 10 μg/mL.[25,26] Often, these techniques require several steps of postisolation purification and analysis to ensure the complete removal of contaminating DNA. For example, a common technique involves running the isolated RNA on a 2% agarose gel to identify any contaminating DNA followed by the incubation of RNA with DNase1 to digest the former.[25] The enzyme (DNase 1) is then heat inactivated at 65 °C in the presence of the chelating agent EDTA, which serves to prevent RNA hydrolysis at the higher temperature.[25] Each additional step requires valuable time and also leads to loss of some of the RNA product. These additional steps also introduce the possibility of degradaing the notoriously unstable RNA. Employing DNase 1:AuNC hybrid systems synthesized in the present study would allow simultaneous detection and digestion of contaminating DNA, thus potentially reducing the time and cost and enhancing the yield of RNA isolation.

SUMMARY

In summary, we have been able to create a multifunctional bio-nano hybrid system. Utilizing the reducing properties of proteins as well as active stabilizers for metal nanoclusters, we were able to synthesize blue (Au_8) and red (Au_{25}) emitting DNase 1:AuNCs in addition to DNase 1 stabilized AuNCs containing mixed populations of both Au_8 and Au_{25} clusters in a concentration-dependent fashion. All of the DNase 1:AuNC synthesis products retain the endodeoxyribonuclease activity of

dx.doi.org/10.1021/ac5005794 | Anal. Chem. 2014, 86, 7377−7382

the native enzyme and are able to detect a lower limit of 2 μg/mL of DNA. This limit of detection (LOD) is relevant to real world applications in RNA analysis because the DNA contamination in such samples can be up to 10 μg/mL, which is 5-fold higher than our LOD. The synthesized DNase 1:NCs could be potentially used for simultaneous detection and digestion of contaminating DNA in the RNA isolation process.

■ ASSOCIATED CONTENT

Supporting Information

Additional experimental details and control experiments. This material is available free of charge via the Internet at http://pubs.acs.org.

■ AUTHOR INFORMATION

Corresponding Author

*A. L. West. E-mail: abby.west2.ctr@mail.mil.

Author Contributions

The paper was written through contributions of all authors. All authors have given approval to the final version of the paper.

Notes

The authors declare no competing financial interest.

■ ACKNOWLEDGMENTS

The authors thank V. Rodriguez Santiago for the X-ray photoelectron spectroscopy. For transmission electron microscopy (TEM) analysis, we acknowledge the support of the Maryland NanoCenter and its NispLab. The NispLab is supported in part by the NSF as a MRSEC Shared Experimental Facility. The authors also thank M. Sellers and J. Martin for aid and input on this work. A. West acknowledges the receipt of an ARL-ORAU Postdoctoral Associateship. D.P.C. is a contractor to the U.S. Army Research Laboratory under contract NNL09AA00A.

■ REFERENCES

(1) Zheng, J.; Nicovich, P. R.; Dickson, R. M. *Annu. Rev. Phys. Chem.* **2007**, *58*, 409.

(2) Zheng, J.; Zhang, C.; Dickson, R. M. *Phys. Rev. Lett.* **2004**, *93*, 077402.

(3) Alivisatos, A. P. *Science* **1996**, *271*, 933.

(4) Chen, C. T.; Chen, W. J.; Liu, C. Z.; Chang, L. Y.; Chen, Y. C. *Chem. Commun. (Camb)* **2009**, 7515.

(5) Chen, W. Y.; Lin, J. Y.; Chen, W. J.; Luo, L. Y.; Diau, E. W. G.; Chen, Y. C. *Nanomedicine* **2010**, *5*, 755.

(6) Shang, L.; Dong, S. J.; Nienhaus, G. U. *Nano Today* **2011**, *6*, 401.

(7) Shang, L.; Dorlich, R. M.; Brandholt, S.; Schneider, R.; Trouillet, V.; Bruns, M.; Gerthsen, D.; Nienhaus, G. U. *Nanoscale* **2011**, *3*, 2009.

(8) Shang, L.; Dorlich, R. M.; Brandholt, S.; Azadfar, N.; Nienhaus, G. U. *Proc. SPIE* **2012**, *8232*, 82321J.

(9) Zhang, A.; Tu, Y.; Qin, S.; Li, Y.; Zhou, J.; Chen, N.; Lu, Q.; Zhang, B. *J. Colloid Interface Sci.* **2012**, *372*, 239.

(10) Chan, P. H.; Ghosh, B.; Lai, H. Z.; Peng, H. L.; Mong, K. K.; Chen, Y. C. *PLoS One* **2013**, *8*, e58064.

(11) Chen, H.; Li, B.; Wang, C.; Zhang, X.; Cheng, Z.; Dai, X.; Zhu, R.; Gu, Y. *Nanotechnology* **2013**, *24*, 055704.

(12) Xie, J.; Zheng, Y.; Ying, J. Y. *J. Am. Chem. Soc.* **2009**, *131*, 888.

(13) Le Guevel, X.; Daum, N.; Schneider, M. *Nanotechnology* **2011**, *22*, 275103.

(14) Kawasaki, H.; Hamaguchi, K.; Osaka, I.; Arakawa, R. *Adv. Funct Mater.* **2011**, *21*, 3508.

(15) Wei, H.; Wang, Z.; Yang, L.; Tian, S.; Hou, C.; Lu, Y. *Analyst* **2010**, *135*, 1406.

(16) Liu, C. L.; Wu, H. T.; Hsiao, Y. H.; Lai, C. W.; Shih, C. W.; Peng, Y. K.; Tang, K. C.; Chang, H. W.; Chien, Y. C.; Hsiao, J. K.; Cheng, J. T.; Chou, P. T. *Angew. Chem., Int. Ed.* **2011**, *50*, 7056.

(17) Wen, F.; Dong, Y. H.; Feng, L.; Wang, S.; Zhang, S. C.; Zhang, X. R. *Anal. Chem.* **2011**, *83*, 1193.

(18) Chen, Y.; Wang, Y.; Wang, C.; Li, W.; Zhou, H.; Jiao, H.; Lin, Q.; Yu, C. *J. Colloid Interface Sci.* **2013**, *396*, 63.

(19) Garcia, A. R.; Rahn, I.; Johnson, S.; Patel, R.; Guo, J.; Orbulescu, J.; Micic, M.; Whyte, J. D.; Blackwelder, P.; Leblanc, R. M. *Colloids Surf., B* **2013**, *105*, 167.

(20) Chevrier, D. M.; Chatt, A.; Zhang, P. *J. Nanophotonics* **2012**, *6*, 064504.

(21) Zhang, H.; Liu, Q.; Wang, T.; Yun, Z.; Li, G.; Liu, J.; Jiang, G. *Anal. Chim. Acta* **2013**, *770*, 140.

(22) Selvakannan, P. R.; Swami, A.; Srisathiyanarayanan, D.; Shirude, P. S.; Pasricha, R.; Mandale, A. B.; Sastry, M. *Langmuir* **2004**, *20*, 7825.

(23) Chen, T. H.; Tseng, W. L. *Small* **2012**, *8*, 1912.

(24) Pruvost, M.; Grange, T.; Geigl, E. M. *Biotechniques* **2005**, *38*, 569.

(25) Tondeur, S.; Agbulut, O.; Menot, M. L.; Larghero, K.; Paulin, D.; Menasche, P.; Sarnuel, J. L.; Chomienne, C.; Cassinat, B. *Mol. Cell. Probes* **2004**, *18*, 437.

(26) Matthews, J. L.; Chung, M.; Matyas, R. J. *Biotechniques* **2002**, *32*, 1412.

(27) Anez-Lingerfelt, M.; Fox, G. E.; Willson, R. C. *Anal. Biochem.* **2009**, *384*, 79.